photonics

Communication

Enhanced Spin Hall Shift by Multipoles of Different Orders in Spherical Particles

Rudao Li [1], Dongliang Gao [1,*] and Lei Gao [1,2,*]

[1] Institute of Theoretical and Applied Physics, School of Physical Science and Technology, Suzhou 215006, China
[2] School of Optical and Electronic Information, Suzhou City University, Suzhou 215104, China
* Correspondence: dlgao@suda.edu.cn (D.G.); leigao@suda.edu.cn (L.G.)

Abstract: The spin–orbit interaction of light is universal in the process of light scattering, and an important aspect is the spin Hall effect. The spin Hall effect of light also exists in a three-dimensional (3D) system. When circularly polarized light is incident on a spherical particle, the transverse displacement of the particle relative to the scattering plane can be observed due to the spiraling of the Poynting vector in the far field. In general, the spin Hall shift of light is negligible and difficult to detect in experiments. In this paper, we use a high-refractive-index (HRI) core-shell structure to excite high-order multipoles and explore the interaction between different order multipoles to enhance the spin Hall shift in the microwave band. We show that there exist some angles that increase the spin Hall shift when two particular multipoles are equal and dominated. Our work provides a new perspective for understanding the interaction between light and particles and enhances the spin Hall shift of the sphere in the microwave band.

Keywords: spin Hall shift of light; core-shell structure; Mie theory; multipoles interaction

1. Introduction

Light carries both spin angular momentum (SAM) and orbit angular momentum (OAM). SAM and OAM interact in the process of light propagation called the spin–orbit interaction (SOI) of light [1–3]. Recently, the SOI of light has attracted enormous attention because it shows the dynamic characteristics of light and spin-to-orbit AM conversion, resulting in various interesting phenomena and applications. In the above phenomenon, the spin Hall effect of light (SHEL) is one of the most active research branches in the SOI of light.

When circularly polarized light is incident on the optical interface between two media, the scattered light will have a tiny displacement compared to the incident light. This tiny displacement is called the SHEL or photonic spin Hall effect (SHE) [4–7]. In 2004, Bliokh et al. used semiclassical theory to explain this phenomenon and named it the Hall effect of light [4]. In 2008, Hosten et al. designed a notable experiment to measure the spin Hall shift and verify the theory [6]. Generally, the SHEL is quite small, but it can be enhanced by metamaterial [8,9], metasurface [10,11], topological edge states [12], or the near Brewster angle [13]. The spin Hall effect of light is applied in identifying graphene layers [14], measuring 2D material optical constants [15], differential microscopy [16], precision metrology [17,18], and so on [1,19]. Under certain conditions, the longitudinal and transverse shifts of the optical beams may be highly anomalous, i.e., larger than the incident wavelength, such as when using space-varying PB phases in homogeneous media [20], exploring exceptional points in PT-symmetric structures [21], or using the singularity in the Berry phase appearing in the beam Fourier spectrum [22].

In the case of a three-dimensional (3D) scatterer, we can also define the spin Hall effect of light [23,24]. In the 3D case, the spin Hall shift [24–26] is caused by the spiral

check for updates

Citation: Li, R.; Gao, D.; Gao, L. Enhanced Spin Hall Shift by Multipoles of Different Orders in Spherical Particles. *Photonics* **2023**, *10*, 732. https://doi.org/10.3390/photonics10070732

Received: 30 April 2023
Revised: 18 June 2023
Accepted: 25 June 2023
Published: 26 June 2023

of the Poynting vector of the scattered light [24,27–30]. Generally, one can use Mie theory and multipole expansion to calculate the shift. Normally, the spin Hall shift of the sphere is negligible on small particles (r $\ll$ λ). In previous work, researchers used dual symmetry [25,31], the core-shell structure [32], the topological magnetoelectric effect [33], the graphene-wrapped sphere structure [26], the chiral structure [34], etc., to enhance the SHEL. In addition, researchers have also undertaken work on enhancing the spin Hall shift of the ellipsoidal structure [35,36] and using single closed elliptical nanoslits to observe optical SHE. However, little has been done to enhance the SHEL by exploiting higher multipole interactions.

In this paper, we use the core-shell structure to excite higher-order multipoles to enhance the spin Hall shift in multiple frequency bands in the microwave band. Our theory suggests that there will be some specific angles to enhance the spin Hall shift when two multipoles are equal and dominated. This study provides new insights into understanding the interaction between light and particles and offers new ways to enhance the spin Hall shift of a sphere in the microwave waveband.

2. Structure and Theoretical Formula

We consider a lossless core-shell particle embedded in a vacuum ($\varepsilon = 1$). The core radius r_a is adjustable with a relative permittivity of $\varepsilon_a = 1$, i.e., the core-shell particle is a hollow particle. The total radius $r = 12$ mm and the permittivity of the shell $\varepsilon_b = 10.5$. Both the core and shell consist of homogeneous non-magnetic media ($\mu = 1$). This structure can stimulate a higher electric/magnetic mode and strongly enhance the spin Hall shift reported in preview work [32,37–39]. The incident light is a circular plane wave with wave number ($k = \frac{2\pi}{\lambda}$), carrying a spin of $\sigma = \pm 1$, depending on the left/right polarization state (a schematic diagram is illustrated in Figure 1).

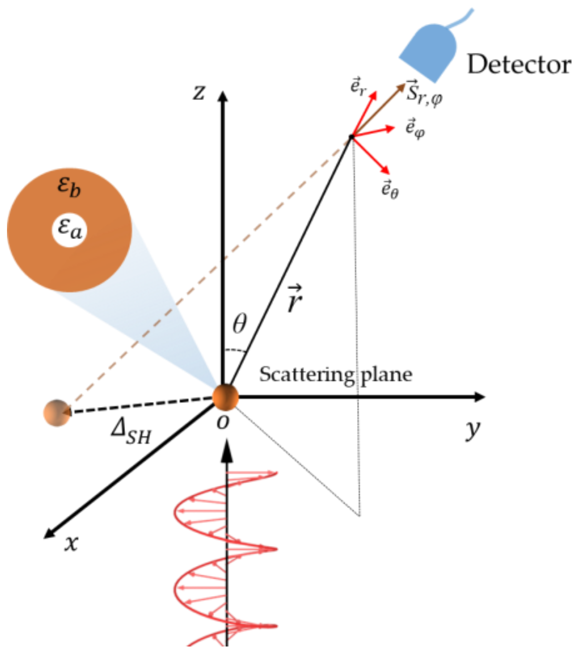

Figure 1. Geometry of spin Hall (SH) shift (Δ) of a spherical core-shell particle. The incident light is circularly polarized. $\vec{r}$ is the position from the origin to the observation point. $\vec{S}_{r,\varphi}$ is the component of the Poynting vector in the plane of $\vec{e}_r$ and $\vec{e}_\varphi$. The scattering plane is defined by $\vec{e}_r$ and $\vec{e}_\theta$ and θ is the scattering angle. The spin Hall shift is marked with a black dotted arrow perpendicular to the scattering plane. The permittivity of the core is ε_a and the permittivity of the shell is ε_b.

We use multiple Mie expansions to solve this scattered problem. We consider a monochromatic left-handed circular plane wave of the form $\overrightarrow{E}_i^L = E_0 e^{ikz}\left(\overrightarrow{e}_x - i\overrightarrow{e}_y\right)e^{-i\omega t}$. The $e^{-i\omega t}$ is the time-harmonic factor and can be reduced in the calculation. We may expand the incident light in a vector spherical harmonics function.

$$\overrightarrow{E}_i^L = \sum_{n=1}^{\infty} E_n \left(\overrightarrow{M}_{o1n}^{(1)} - i\overrightarrow{N}_{e1n}^{(1)} - i\overrightarrow{M}_{e1n}^{(1)} + \overrightarrow{N}_{e1n}^{(1)} \right) \tag{1}$$

$$\overrightarrow{H}_i^L = -\frac{k}{\omega\mu} \sum_{n=1}^{\infty} E_n \left(\overrightarrow{M}_{o1n}^{(1)} + i\overrightarrow{N}_{o1n}^{(1)} + i\overrightarrow{M}_{o1n}^{(1)} + \overrightarrow{N}_{e1n}^{(1)} \right) \tag{2}$$

where $E_n = E_0 i^n (2n+1)/(n(n+1))$, $\overrightarrow{M}_{\mathrm{o1n}}^{(1)}$, $\overrightarrow{N}_{\mathrm{e1n}}^{(1)}$, $\overrightarrow{M}_{\mathrm{o1n}}^{(1)}$, $\overrightarrow{N}_{\mathrm{o1n}}^{(1)}$ are the vector spherical harmonics functions; the superscript (1) means the generating function is the spherical Bessel function of the first kind [40].

Similarly, we also expand the scattered field in the vector spherical harmonics function,

$$\overrightarrow{E}_s^L = \sum_{n=1}^{\infty} E_n \left(ia_n \overrightarrow{N}_{e1n}^{(3)} - b_n \overrightarrow{M}_{o1n}^{(3)} - ia_n \overrightarrow{N}_{o1n}^{(3)} + ib_n \overrightarrow{M}_{e1n}^{(3)} \right) \tag{3}$$

$$\overrightarrow{H}_s^L = \frac{k}{\omega\mu} \sum_{n=1}^{\infty} E_n \left(ib_n \overrightarrow{N}_{o1n}^{(3)} + ia_n \overrightarrow{M}_{e1n}^{(3)} + b_n \overrightarrow{N}_{e1n}^{(3)} + ia_n \overrightarrow{M}_{o1n}^{(3)} \right) \tag{4}$$

The superscript (3) means the generating function is the spherical Bessel function of the third kind, and a_n, b_n are the scattering coefficients of the core-shell structure. By applying boundary conditions in the two interfaces ($r = r_a$ and $r = r_b$), we obtain the expression of the scattering coefficients a_n, b_n. We define the spin Hall shift of light as the transverse deflection observed in the far field, via the azimuthal component of the Poyning vector as [24]:

$$\Delta_{\mathrm{SH}} = \lim_{r\to\infty} r \left(\frac{S_\phi \overrightarrow{e}_\phi}{|S_r|} \right) \tag{5}$$

where S_r and S_ϕ are the azimuthal and radial components of the scattered Poynting vector $S = \frac{1}{2} * Re\{E_s \times H_s^*\}$. We can see in the expression that the direction of the spin Hall shift is perpendicular to the scattering plane. The physical origin of the spin Hall shift is the spiral of the Poynting vector. The incident CPL has a spin ($\sigma = \pm 1$) because of the SOI in the scattering process, the scattering Poynting vector has a component perpendicular to the radial direction causing a displacement of the spherical particles.

By solving the component of the Poynting vector, the spin Hall shift can be written as [19]:

$$\Delta_{\mathrm{SH}} = \frac{\sigma}{k} \left(\frac{\left| Re\left(S_1^* \left[\sum_{n=1}^{\infty} (2n+1) a_n \pi_n\right] + S_2 \left[\sum_{n=1}^{\infty} (2n+1) b_n \pi_n\right] \right) \right|}{|S_1|^2 + |S_2|^2} \right) \tag{6}$$

where $\sigma = \pm 1$ for the LCP and RCP state. S_1 and S_2 are the amplitude scattering matrix elements defined as:

$$\mathrm{S}_1 = \sum_{n=1}^{\infty} \frac{2n+1}{n(n+1)} (a_n \pi_n + b_n \tau_n) \tag{7}$$

$$\mathrm{S}_2 = \sum_{n=1}^{\infty} \frac{2n+1}{n(n+1)} (a_n \tau_n + b_n \pi_n) \tag{8}$$

$\pi_n(cos\theta)$ and $\tau_n(cos\theta)$ are the angle-dependent functions defined as $\pi_n(cos\theta) = P_n^1(cos\theta)/sin\theta$, $\tau_n(cos\theta) = dP_n^1(cos\theta)/d\theta$. It can be calculated using the associated Legendre function recursion.

3. Simulation Result

In this section, we investigate how core radius change causes change in the spin Hall shift and theoretically analyze how different multipole interactions induce enhancement of the spin Hall shift for a core-shell sphere. We also investigate how core radius change causes change in the spin Hall shift.

In previous work [23,25], we found that, when the electric or magnetic dipole is dominant, the maximum SH shift is λ/π. High refractive index (HRI) spherical particles can provide higher-order multipoles in different frequency bands [38,39,41,42]. We plot the first three scattering coefficients and the SH shift of the core-shell structure; the core radium r_a is 4 mm. The value of the spin Hall shift (Δ_{SH}) is divided by the wavelength (λ).

Figure 2a illustrates that the electric and magnetic multipoles are enhanced at 3 GHz to 9 GHz. Due to the interaction between different poles, the spin Hall shift will be enhanced significantly around multiple frequencies at different scattering angles, as shown in Figure 2b. Thanks to the core-shell structure there is abundant freedom to adjust. Here, we plot the spin Hall shift as it varies with different core radii.

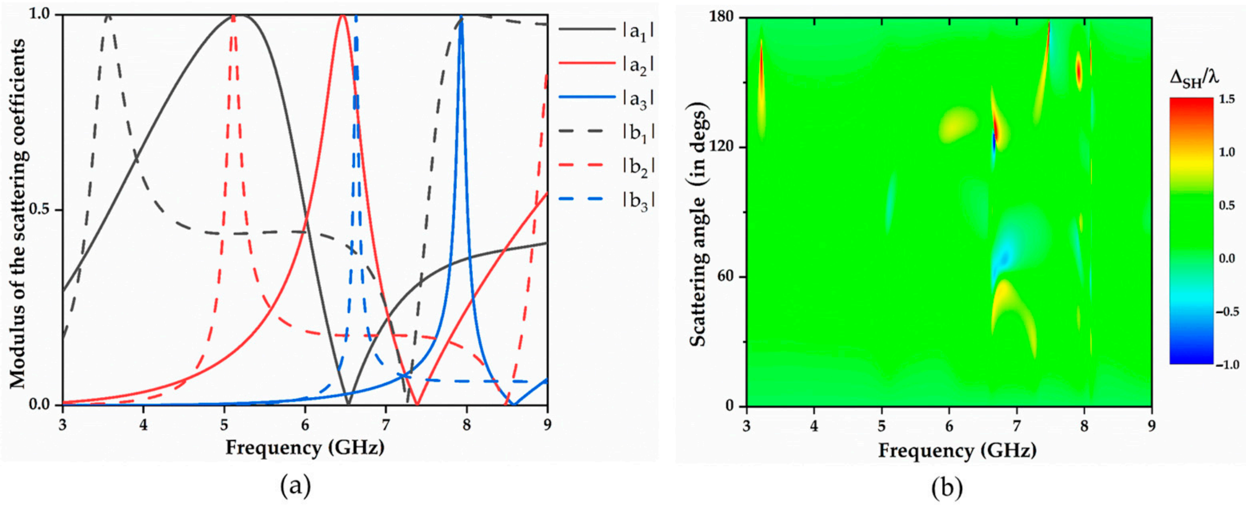

Figure 2. The total radius of sphere $r = 12$ mm. The core radius $r_a = 4$ mm with a permittivity $\varepsilon_a = 1$. The dielectric shell has a permittivity of $\varepsilon_b = 10.5$. (**a**) The first three scattering coefficients of the Mie term. The solid line and dash line represent the contribution of the electric and magnetic multipole, respectively. (**b**) Spin Hall shift of the core-shell structure varies with frequency and scattering angle.

From Equation (6), we know that the spin Hall shift is related to the scattering coefficients of different modes. By changing the core radius, one can make the peak of the scattering coefficients move. The line shapes of the scattering coefficients are shifted differently for different modes causing the peak position of the spin Hall shift to appear, disappear or move. We observe that, in Figure 3d when $r_a = 6$ mm, the frequency around 8.26 GHz and $\theta = \frac{\pi}{2}$, Δ_{SH} is about 1.5 λ; it is easy to design experiments to observe the spin Hall shift. It is also noted that the enhancement of Δ_{sh} is sometimes due to the interaction of multipole modes; for example, the enhancement around 5.3 GHz is related to the electric dipole (a_1), the magnetic dipole (b_1) and the magnetic quadrupole (b_2). Such a case is complicated to show in equations, and we will discuss it in our future work.

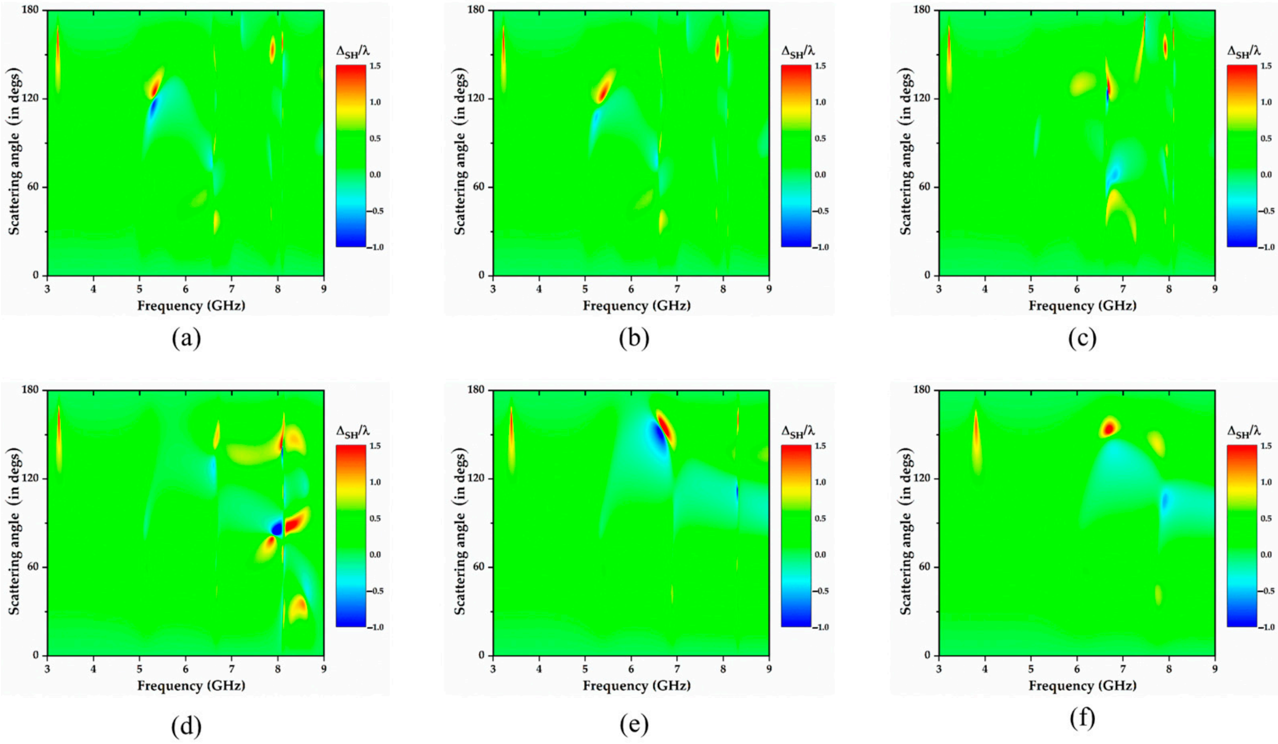

Figure 3. Spin Hall shift with frequency and scattering angle at different core radii. The permittivity of the core is 1 and the permittivity of the shell is 10.5. (**a**) $r_a = 0$ mm; (**b**) $r_a = 2$ mm; (**c**) $r_a = 4$ mm; (**d**) $r_a = 6$ mm; (**e**) $r_a = 8$ mm; (**f**) $r_a = 10$ mm.

3.1. Overlap of Electric Dipole and Magnetic Dipole

In the case that an electric dipole (a_1) and magnetic dipole (b_1) are dominated, substitute the value of τ_1 and π_1 into Equations (7) and (8) (the denominator of the spin Hall shift). These reduce to:

$$\frac{3}{2}a_1 + \frac{3}{2}b_1 cos\theta = 0 \tag{9}$$

$$\frac{3}{2}a_1 cos\theta + \frac{3}{2}b_1 = 0 \tag{10}$$

The maximum spin Hall shift can be obtained if the denominator of the expression is close to 0. It is apparent when $a_1 = b_1$ (dual symmetry) and $\theta \approx \pi$, the condition is satisfied. We plot the real part and the imaginary parts of a_1 and b_1 as well as the value of the spin Hall shift from 3 GHz to 3.5 GHz for different core radii.

Figure 4 illustrates when the scattering coefficients a_1 and b_1 are equal and the scattering angle (θ) is around $\theta \approx \pi$. Previous research work has found that, in dual symmetry ($a_1 = b_1$), the spin Hall shift can be enhanced. Our work produced the same result—the spin Hall shift is enhanced significantly by about 1.5 λ. We also change the core radius of the core-shell structure. Figure 4a–c show that increase in the core radius causes the position of $a_1 = b_1$ to undergo a blue shift. As a result, the enhanced position of the spin Hall shift also has a blue shift, while the enhancement of the spin Hall shift remains around 1.5 λ.

3.2. Overlap of Electric Quadrupole and Magnetic Octupole

In the case that the electric quadrupole (a_2) and magnetic octupole (b_3) are dominant, substituting the corresponding value of τ_n and π_n into Equations (6) and (7), they reduce to:

$$S_1 = \frac{5}{2}a_2 cos\theta + \frac{7}{12}b_3\left(6cos\theta - \frac{45}{2}\sin^2\theta cos\theta\right) \tag{11}$$

$$S_2 = \frac{5}{2}a_2 cos2\theta + \frac{7}{12}b_3(6 - \frac{15}{2}\sin^2\theta) \quad (12)$$

The denominator of the spin Hall shift $D = |S_1|^2 + |S_2|^2$. Considering $a_2 \approx b_3$, when D is close to 0, the spin Hall shift has a maximum value. So, the denominator can be further simplified to the following form:

$$D = \left|\frac{5}{2}cos\theta + \frac{7}{12}(6cos\theta - \frac{45}{2}\sin^2\theta cos\theta)\right|^2 + \left|\frac{5}{2}cos2\theta + \frac{7}{12}\left(6 - \frac{15}{2}\sin^2\theta\right)\right|^2 \approx 0 \quad (13)$$

$$0 \leq \theta \leq \pi \quad (14)$$

It is notable that a_2 and b_3 do not appear in the equations. In other words, if a_2 and b_3 are equal at a certain frequency and the equation has a solution, the spin Hall shift should be enhanced at a certain angle.

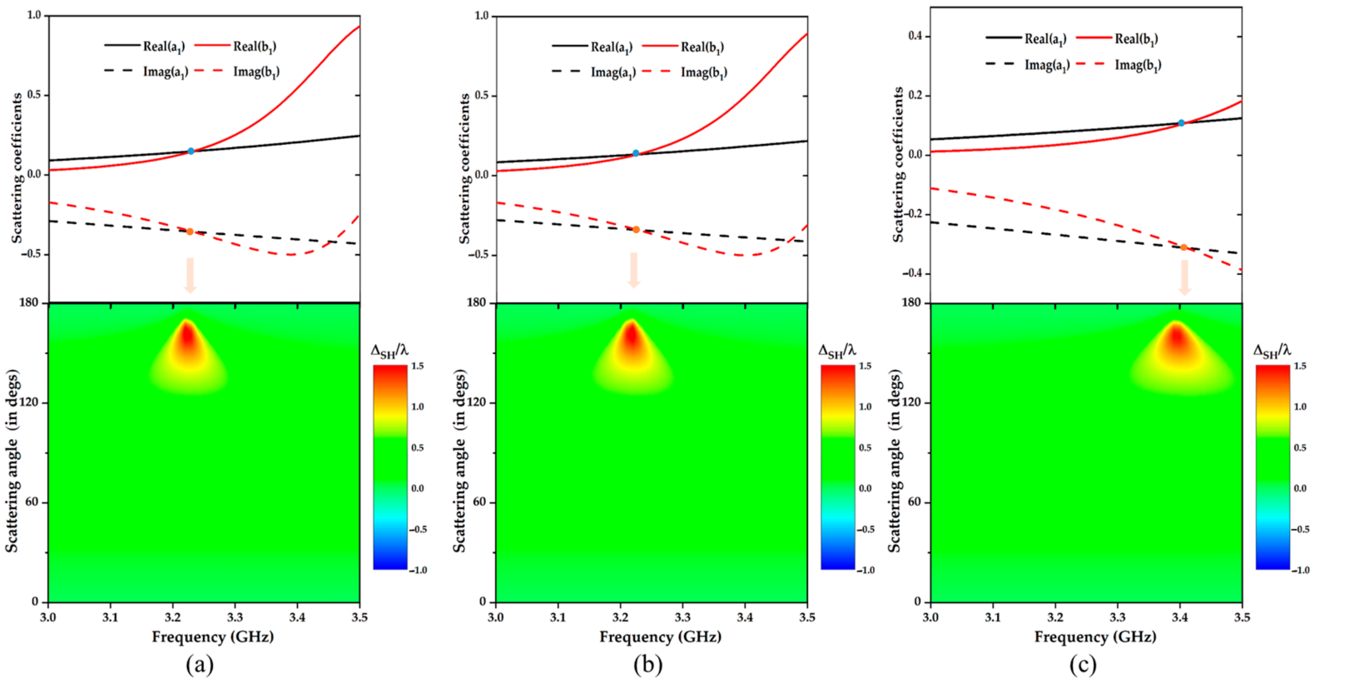

Figure 4. The real and imaginary parts of the scattering coefficient a_1 and b_1 vary with frequency, and the spin Hall shift varies with the frequency and scattering angle. The frequency ranges from 3 GHz to 3.5 GHz. (**a**) $r_a = 2$ mm; (**b**) $r_a = 4$ mm; (**c**) $r_a = 8$ mm; The black dotted line and red dotted line represent the imaginary parts of a_1 and b_1 The blue and orange dots mark where the real and imaginary parts of a_1 and b_1 are equal, respectively.

The scattering angles satisfying the conditions are about 49° and 132°; the denominator has a local minimum in these two angles. We plot the real part and imaginary parts of a_2 and b_3 as well as the value of the spin Hall shift from 6.5 GHz to 7 GHz. We also plot the spin Hall shift as a function of the angle at 6.66 GHz, considering only a_2 and b_3 and considering the first six multipoles. We also plot the variation in the numerator and denominator of the spin Hall shift expression with an angle when only a_2 and b_3 are considered.

Figure 5a shows that the spin Hall shift enhances and splits around the scattering angles satisfying the equation (49° and 132°) at the position where a_2 and b_3 are equal. The incident frequency in Figure 5b is 6.66 GHz. The above figure shows that only the considered a_2 and b_3 provide a good fit to the spin Hall shift as a function of angle. The figure below shows that, at the position where the denominator is the minimum, the numerator tends to zero faster than the parent, so the position where the spin Hall shift is the maximum is not exactly in the position where the denominator is the minimum. Notably, there is a conversion from positive to negative in the numerator at the position where the denominator is the minimum, causing the spin Hall shift to have a split around the denominator minimum position.

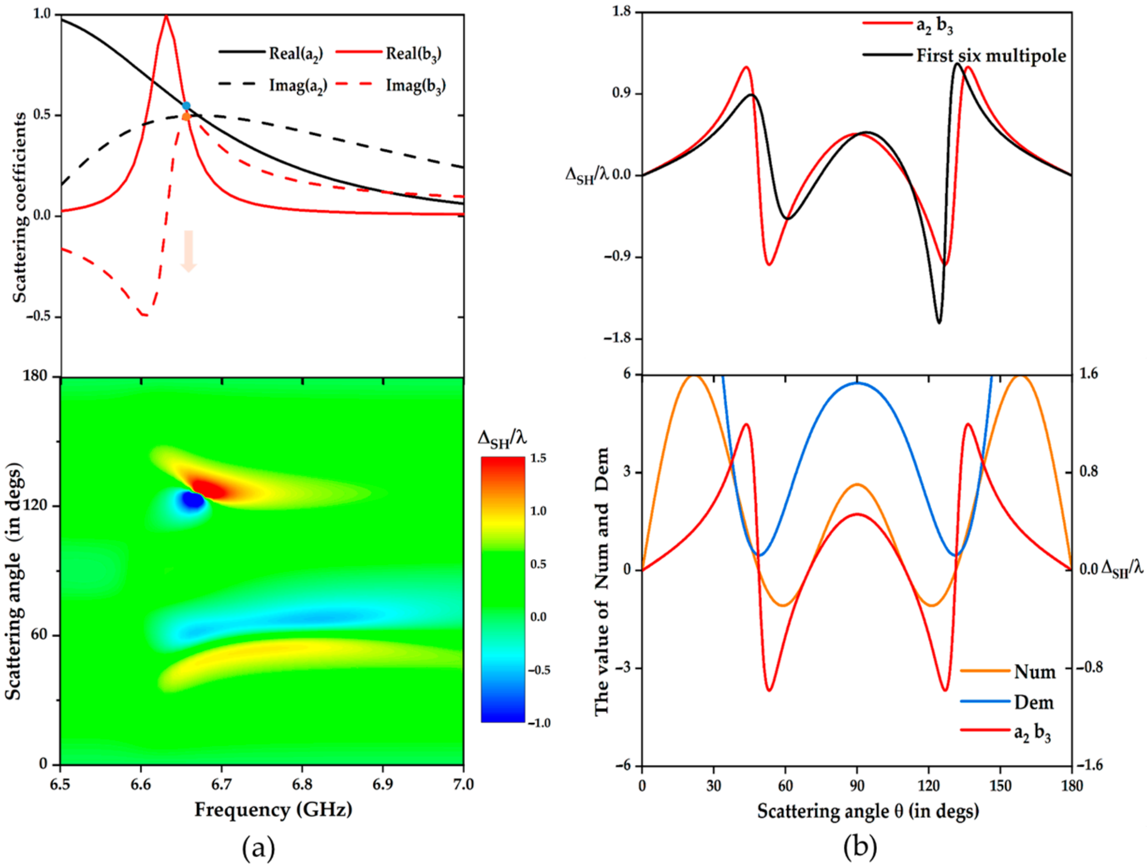

Figure 5. Parameters of core-shell structure: the core radius is 4 mm with a permittivity of 1 and the shell radius is 12.5 mm with a permittivity of 10.5. (**a**) The figure above shows the scattering coefficients a_2 and b_3 as they vary with frequency, with the blue and orange dots representing the positions where the real and imaginary parts of the scattering coefficients are equal, respectively. The figure below shows the spin Hall shift as a function of the frequency and scattering angle. (**b**) The frequency is 6.66 GHz. The figure above shows the spin Hall shift as a function of angle. The red solid line and the black solid line represent the case where only a_2 and b_3 are considered and the case where the first six multipoles are considered, respectively.

3.3. Overlap of Electric Octupole and Magnetic Dipole

In the case that the electric octupole (a_3) and the magnetic dipole (b_1) are dominated, substitute the corresponding value of τ_n and π_n into Equations (6) and (7). This reduces to:

$$S_1(cos\theta) = \frac{7}{12}a_3\left(6 - \frac{15}{2}\sin^2\theta\right) + \frac{3}{2}b_1 cos\theta \tag{15}$$

$$S_2(cos\theta) = \frac{7}{12}a_3\left(6cos\theta - \frac{45}{2}\sin^2\theta cos\theta\right) + \frac{3}{2}b_1 \tag{16}$$

The denominator of the spin Hall shift $D = |S_1|^2 + |S_2|^2$. Considering $a_3 \approx b_1$, when D is close to the minimal value, the spin Hall shift has a maximum value. So, the denominator can be further simplified to the following form:

$$D = |a_3|^2\left(\left|\frac{7}{12}\left(6-\frac{15}{2}\sin^2\theta\right)+\frac{3}{2}cos\theta\right|^2+\left|\frac{5}{2}cos2\theta+\frac{7}{12}(6-\frac{15}{2}\sin^2\theta)\right|\right) \quad (17)$$

$$0 \le \theta \le \pi \quad (18)$$

Similarly, the denominator minimum position is independent of the value of a_3 and b_1. The scattering angles satisfying the conditions are 80° and 155°.The spin Hall shift should be enhanced around these two angles. We plot the values of the real and imaginary parts of a_3 and b_1 and the corresponding spin Hall shifts when the radii of the cores are 2 mm, 4 mm, and 8 mm. The frequency range is from 7.5 GHz to 8 GHz.

As is shown in Figure 6, the spin Hall shift is significantly enhanced around 155° at 7.92 GHz ($a_3 \approx b_1$) when the core radii are 2 mm and 4 mm. However, the enhancement of the spin Hall shift is not obvious around 80° because the values of the other multipoles are also large and contribute to the spin Hall shift. When the core radius is 8 mm, the values of a_3 and b_1 are not equal from 7.5 GHz to 8 GHz. Although the spin Hall shift enhances slightly, this is not caused by the dominance of a_3 and b_1.

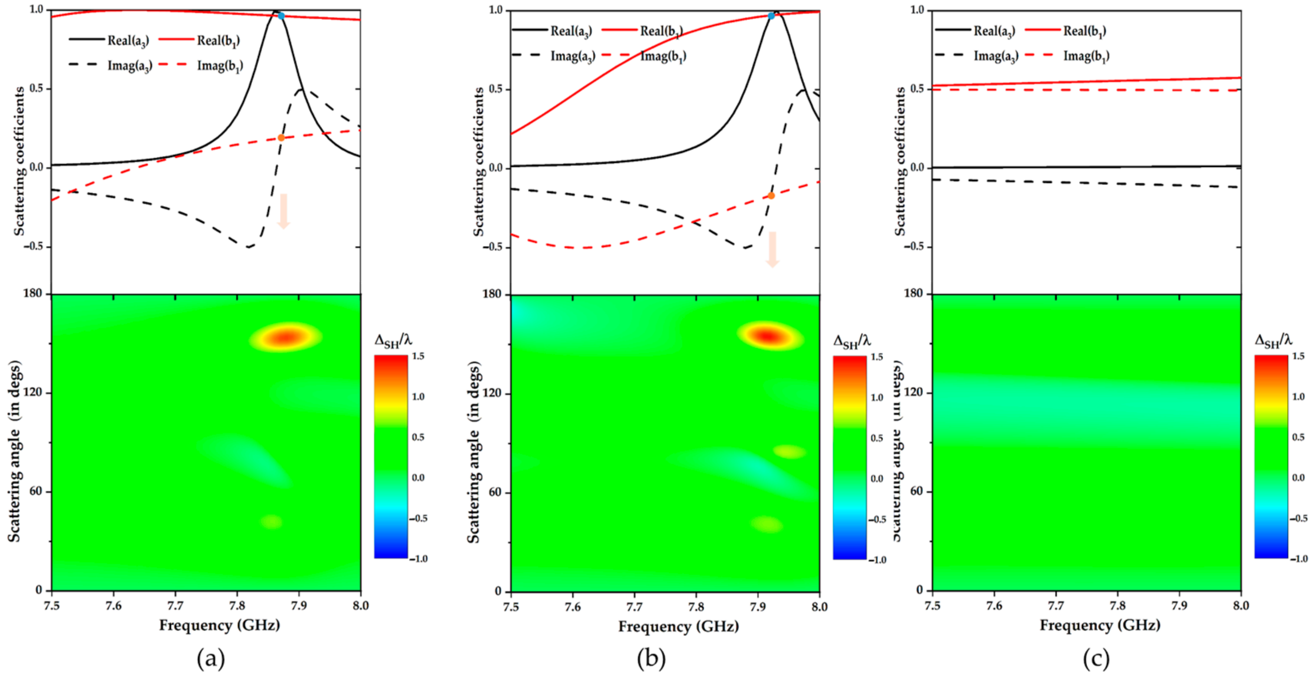

Figure 6. Parameters of core-shell structure: the permittivity of the core is 1 and the permittivity of the shell is 10.5. The radius of the core-shell structure is 12.5 mm, and the radii of the cores are (**a**) 2 mm, (**b**) 4 mm, and (**c**) 8 mm. The figure at the top represents the variation in the real and imaginary parts of a_3 and b_1 with frequency. The black solid line and red solid line represent the real parts of a_3 and b_1. The black dotted line and red dotted line represent the imaginary parts of a_3 and b_1. The figure at the bottom represents the spin Hall shift with frequency and angle. The frequency ranges from 7.5 GHz to 8 GHz.

4. Conclusions

In this paper, we investigate enhancement of the spin Hall shift of high refractive index core-shell spherical particles (hollow particles) in the microwave band based on Mie theory. We use the fact that high refractive index core-shell particles can excite higher-order multipoles and enhance the spin Hall shift of the core-shell structure through overlapping multipoles of different orders, generalizing the work of previous researchers. In the condition that certain multipoles are equal and dominant, we reveal that the enhanced position of the spin Hall shift is only related to the angle. Our work provides a theoretical basis for designing experiments to observe the spin Hall shift of microwave-band spherical particles. The spin Hall shift of light can also be observed in experiments in the far field. The change in the transversal shifts can be easily detected by flipping the helicity of the incident light [36]. We expect that our work will contribute to the design and optimization of microwave optical devices and to the understanding of spin–orbit interactions of light.

Author Contributions: Conceptualization, D.G. and L.G.; methodology, D.G.; software, R.L.; investigation R.L.; writing—original draft preparation, R.L.; writing—review and editing, D.G. and L.G.; visualization, R.L.; supervision, D.G. and L.G.; funding acquisition, L.G. All authors have read and agreed to the published version of the manuscript.

Funding: The authors gratefully acknowledge financial support from the National Natural Science Foundation of China (Grant Nos. 92050104, 12274314), Natural Science Foundation of Jiangsu Province (Grant No. BK20221240).

Institutional Review Board Statement: Not applicable.

Informed Consent Statement: Not applicable.

Data Availability Statement: The data that support the findings of this study are available from the corresponding author upon reasonable request.

Conflicts of Interest: The authors declare no conflict of interest.

References

1. Ling, X.; Zhou, X.; Huang, K.; Liu, Y.; Qiu, C.-W.; Luo, H.; Wen, S. Recent Advances in the Spin Hall Effect of Light. *Rep. Prog. Phys.* **2017**, *80*, 066401. [CrossRef]
2. Bliokh, K.Y.; Rodríguez-Fortuño, F.J.; Nori, F.; Zayats, A.V. Spin–Orbit Interactions of Light. *Nat. Photonics* **2015**, *9*, 796–808. [CrossRef]
3. Bliokh, K.Y.; Nori, F. Transverse and Longitudinal Angular Momenta of Light. *Phys. Rep.* **2015**, *592*, 1–38. [CrossRef]
4. Onoda, M.; Murakami, S.; Nagaosa, N. Hall Effect of Light. *Phys. Rev. Lett.* **2004**, *93*, 083901. [CrossRef] [PubMed]
5. Bliokh, K.Y.; Bliokh, Y.P. Conservation of Angular Momentum, Transverse Shift, and Spin Hall Effect in Reflection and Refraction of an Electromagnetic Wave Packet. *Phys. Rev. Lett.* **2006**, *96*, 073903. [CrossRef] [PubMed]
6. Hosten, O.; Kwiat, P. Observation of the Spin Hall Effect of Light via Weak Measurements. *Science* **2008**, *319*, 787–790. [CrossRef]
7. Xiang, Y.; Jiang, X.; You, Q.; Guo, J.; Dai, X. Enhanced Spin Hall Effect of Reflected Light with Guided-Wave Surface Plasmon Resonance. *Photonics Res.* **2017**, *5*, 467. [CrossRef]
8. Tang, T.; Li, C.; Luo, L. Enhanced Spin Hall Effect of Tunneling Light in Hyperbolic Metamaterial Waveguide. *Sci. Rep.* **2016**, *6*, 30762. [CrossRef]
9. Fu, Y.-Y.; Fei, Y.; Dong, D.-X.; Liu, Y.-W. Photonic Spin Hall Effect in PT Symmetric Metamaterials. *Front. Phys.* **2019**, *14*, 62601. [CrossRef]
10. Yin, X.; Ye, Z.; Rho, J.; Wang, Y.; Zhang, X. Photonic Spin Hall Effect at Metasurfaces. *Science* **2013**, *339*, 1405–1407. [CrossRef]
11. Kim, M.; Lee, D.; Yang, Y.; Kim, Y.; Rho, J. Reaching the Highest Efficiency of Spin Hall Effect of Light in the Near-Infrared Using All-Dielectric Metasurfaces. *Nat. Commun.* **2022**, *13*, 2036. [CrossRef] [PubMed]
12. Slobozhanyuk, A.P.; Poddubny, A.N.; Sinev, I.S.; Samusev, A.K.; Yu, Y.F.; Kuznetsov, A.I.; Miroshnichenko, A.E.; Kivshar, Y.S. Enhanced Photonic Spin Hall Effect with Subwavelength Topological Edge States. *Laser Photonics Rev.* **2016**, *10*, 656–664. [CrossRef]
13. Luo, H.; Zhou, X.; Shu, W.; Wen, S.; Fan, D. Enhanced and Switchable Spin Hall Effect of Light near the Brewster Angle on Reflection. *Phys. Rev. A* **2011**, *84*, 043806. [CrossRef]
14. Zhou, X.; Ling, X.; Luo, H.; Wen, S. Identifying Graphene Layers via Spin Hall Effect of Light. *Appl. Phys. Lett.* **2012**, *101*, 251602. [CrossRef]
15. Chen, S.; Zhou, X.; Ling, X.; Shu, W.; Luo, H.; Wen, S. Measurement of the Optical Constants of Monolayer MoS_2 via the Photonic Spin Hall Effect. *Appl. Phys. Lett.* **2021**, *118*, 111104. [CrossRef]
16. Wang, R.; He, S.; Luo, H. Photonic Spin-Hall Differential Microscopy. *Phys. Rev. Appl.* **2022**, *18*, 044016. [CrossRef]
17. Zhou, X.; Xiao, Z.; Luo, H.; Wen, S. Experimental Observation of the Spin Hall Effect of Light on a Nanometal Film via Weak Measurements. *Phys. Rev. A* **2012**, *85*, 043809. [CrossRef]
18. Qiu, X.; Zhou, X.; Hu, D.; Du, J.; Gao, F.; Zhang, Z.; Luo, H. Determination of Magneto-Optical Constant of Fe Films with Weak Measurements. *Appl. Phys. Lett.* **2014**, *105*, 131111. [CrossRef]

19. Kotlyar, V.V.; Stafeev, S.S.; Kozlova, E.S.; Nalimov, A.G. Spin-Orbital Conversion of a Strongly Focused Light Wave with High-Order Cylindrical–Circular Polarization. *Sensors* **2021**, *21*, 6424. [CrossRef]
20. Zhu, W.; Zheng, H.; Zhong, Y.; Yu, J.; Chen, Z. Wave-Vector-Varying Pancharatnam-Berry Phase Photonic Spin Hall Effect. *Phys. Rev. Lett.* **2021**, *126*, 083901. [CrossRef]
21. Zhou, X.; Lin, X.; Xiao, Z.; Low, T.; Alù, A.; Zhang, B.; Sun, H. Controlling Photonic Spin Hall Effect via Exceptional Points. *Phys. Rev. B* **2019**, *100*, 115429. [CrossRef]
22. Mazanov, M.; Yermakov, O.; Bogdanov, A.; Lavrinenko, A. On Anomalous Optical Beam Shifts at Near-Normal Incidence. *APL Photonics* **2022**, *7*, 101301. [CrossRef]
23. Haefner, D.; Sukhov, S.; Dogariu, A. Spin Hall Effect of Light in Spherical Geometry. *Phys. Rev. Lett.* **2009**, *102*, 123903. [CrossRef]
24. Mansha, S.; Dutta Gupta, S.; Banerjee, A.; Ghosh, N. Giant Goos–Hänchen Shift in Scattering: The Role of Interfering Localized Plasmon Modes. *Opt. Lett.* **2014**, *39*, 4100. [CrossRef]
25. Gao, D.; Shi, R.; Miroshnichenko, A.E.; Gao, L. Enhanced Spin Hall Effect of Light in Spheres with Dual Symmetry. *Laser Photonics Rev.* **2018**, *12*, 1800130. [CrossRef]
26. Zhang, Q.; Gao, D.L.; Gao, L. Tunable Spin Hall Shift of Light from Graphene-Wrapped Spheres. *Opt. Express* **2021**, *29*, 9816. [CrossRef] [PubMed]
27. Li, X.; Shu, J.; Arnoldus, H.F. Far-Field Detection of the Dipole Vortex. *Opt. Lett.* **2008**, *33*, 2269–2271. [CrossRef] [PubMed]
28. Dogariu, A.; Schwartz, C. Conservation of Angular Momentum of Light in Single Scattering. *Opt. Express* **2006**, *14*, 8425. [CrossRef]
29. Arnoldus, H.F.; Foley, J.T. The Dipole Vortex. *Opt. Commun.* **2004**, *231*, 115–128. [CrossRef]
30. Arnoldus, H.F.; Li, X.; Shu, J. Subwavelength Displacement of the Far-Field Image of a Radiating Dipole. *Opt. Lett.* **2008**, *33*, 1446. [CrossRef]
31. Olmos-Trigo, J.; Sanz-Fernández, C.; García-Etxarri, A.; Molina-Terriza, G.; Bergeret, F.S.; Sáenz, J.J. Enhanced Spin-Orbit Optical Mirages from Dual Nanospheres. *Phys. Rev. A* **2019**, *99*, 013852. [CrossRef]
32. Shi, R.; Gao, D.L.; Hu, H.; Wang, Y.Q.; Gao, L. Enhanced Broadband Spin Hall Effects by Core-Shell Nanoparticles. *Opt. Express* **2019**, *27*, 4808. [CrossRef]
33. Wang, Y.Q.; Hu, H.; Zhang, Q.; Gao, D.L.; Gao, L. Topologically-Tuned Spin Hall Shift around Fano Resonance. *Opt. Express* **2020**, *28*, 21641. [CrossRef] [PubMed]
34. Ali, R. Chirality-Assisted Spin Hall Effect of Light in the Vicinity of the Quasi-Antidual Symmetry Mode of a Chiral Sphere. *Phys. Rev. A* **2022**, *106*, 063508. [CrossRef]
35. Li, W.; Liu, J.; Gao, Y.; Zhou, K.; Liu, S. Photonic Spin Hall Effect on an Ellipsoidal Rayleigh Particle in Scattering Far-Field. *Opt. Express* **2019**, *27*, 28194. [CrossRef] [PubMed]
36. Sun, Y.; Xu, P.; Gao, L.; Miroshnichenko, A.E.; Gao, D. Wavelength-Scale Spin Hall Shift of Light with Morphology-Enhanced Scattering Efficiency from Nanoparticles. *Laser Photonics Rev.* **2022**, *16*, 2200289. [CrossRef]
37. Ruffino, F. Light-Scattering Simulations from Spherical Bimetallic Core–Shell Nanoparticles. *Micromachines* **2021**, *12*, 359. [CrossRef]
38. Liberal, I.; Ederra, I.; Gonzalo, R.; Ziolkowski, R.W. Superbackscattering from Single Dielectric Particles. *J. Opt.* **2015**, *17*, 072001. [CrossRef]
39. Powell, A.W.; Hibbins, A.P.; Sambles, J.R. Multiband Superbackscattering via Mode Superposition in a Single Dielectric Particle. *Appl. Phys. Lett.* **2021**, *118*, 251107. [CrossRef]
40. Bohren, C.F.; Huffman, D.R. *Absorption and Scattering of Light by Small Particles*; Wiley-VCH: Weinheim, Germany, 2004; ISBN 978-0-471-29340-8.
41. Liu, W.; Miroshnichenko, A.E.; Neshev, D.N.; Kivshar, Y.S. Broadband Unidirectional Scattering by Magneto-Electric Core–Shell Nanoparticles. *ACS Nano* **2012**, *6*, 5489–5497. [CrossRef]
42. Liu, W.; Zhang, J.; Lei, B.; Ma, H.; Xie, W.; Hu, H. Ultra-Directional Forward Scattering by Individual Core-Shell Nanoparticles. *Opt. Express* **2014**, *22*, 16178. [CrossRef] [PubMed]